Hum Genet (2005) 118: 508–514
DOI 10.1007/s00439-005-0075-z

SHORT REPORT

**Giles D.J. Watts · Sarju G. Mehta · Chengfeng Zhao
Sheena Ramdeen · Sara Jane Hamilton
Deborah V. Novack · Steven Mumm
Michael P. Whyte · Barbara McGillivray
Virginia E. Kimonis**

Mapping autosomal dominant progressive limb-girdle myopathy with bone fragility to chromosome 9p21-p22: a novel locus for a musculoskeletal syndrome

Received: 6 May 2005 / Accepted: 5 September 2005 / Published online: 22 October 2005

Abstract Progressive myopathy of a limb-girdle distribution and bone fragility is a rare autosomal dominant disorder of unknown etiology. Affected individuals, within this family, present with various combinations of progressive muscle weakness, easy fracturing, and poor healing of long bones. Additional features include premature graying with thin hair, thin skin, hernias, and clotting disorders. Electromyograms show myopathic changes and biopsies reveal non-specific myopathic changes. Skeletal radiographs demonstrate coarse trabeculation, patchy sclerosis, cortical thickening, and narrowing of medullary cavities. We report genetic mapping of this disorder to chromosome 9p21-p22 in a multigenerational family. A genome-wide scan for the disease locus obtained a maximal LOD score of 3.74 for marker GATA87E02 N (D9S1121). Haplotype analysis localized the disease gene within a 15 Mb interval flanked by markers AGAT142P and GATA5E06P. This region also localizes diaphyseal medullary stenosis with malignant fibrous histiocytoma (DMS-MFH). Identification of the disease gene will be necessary to understand the pathogenesis of this complex disorder.

Funding for this study is from the National Institutes of Health NIAMS RO1 AR050236-01A1, R03 AR46869-03, NINDS K02 NS02157 award, the Muscular Dystrophy Association, Paget Foundation, Children's Hospital Boston and Shriners Hospitals for Children.

G. D.J. Watts · S. G. Mehta · S. Ramdeen · V. E. Kimonis (✉)
Division of Genetics and Metabolism, Children's Hospital, Harvard Medical School, 300 Longwood Avenue, Fegan 10, Boston, MA, 02115 USA
E-mail: virginia.kimonis@childrens.harvard.edu
Tel.: +1-617-3556394
Fax: +1-617-7300466

C. Zhao
Center for Medical Genetics, Molecular Genetics Laboratory, 1000 North Oak Avenue, Marshfield, WI, USA

S. J. Hamilton · B. McGillivray
Provincial Medical Genetics Programme, Children's and Women's Health Centre of British Columbia C234, 500 Oak Street, Vancouver, British Columbia, Canada

D. V. Novack
Departments of Pathology and Medicine, Washington University School of Medicine, 660 S. Euclid Avenue, St. Louis, MO, USA

S. Mumm · M. P. Whyte
Division of Bone and Mineral Diseases, Washington University School of Medicine, and Center for Metabolic Bone Disease and Molecular Research, Shriners Hospital for Children, St. Louis, MO, USA

Introduction

Hereditary myopathy of limb-girdle distribution and bone fragility is a rare, complex, and debilitating autosomal dominant disorder (Mehta et al. 2005). The family studied here for genetic mapping was originally reported (Henry et al. 1958) as having autosomal dominant 'limb-girdle muscular dystrophy' with easy fracturability and poor healing of the long bones. Among affected living family members and deceased individuals whose medical records were assessed (three males and four females), 88% of subjects had adult-onset proximal and distal muscle weakness with a mean age at presentation of 29 years, and 77% had fractures and poor healing of major long bones beginning at a mean age of 18 years. Premature graying of hair and thin skin was observed in several individuals. Electromyograms showed early recruitment of small amplitude motor unit potentials and non-specific myopathic changes, and nerve conduction studies were unremarkable. Muscle biopsy specimens revealed non-specific myopathic changes, with no necrotic regenerating fibers, inflammatory infiltrates, or structural abnormalities, and immunohistological stains were normal. Serum creatine phosphokinase levels were normal-to-mildly elevated. Skeletal

radiographs revealed coarse sclerotic trabeculation with cortical thickening and narrow medullary cavities of the long bones. Histopathology of bone showed osteomalacia-like changes in addition to appearances of infarction in some individuals. Fractures were slow to heal. Many affected individuals also had osteomyelitis that was difficult to treat, sometimes leading to amputations.

Materials and methods

Family enrollment

Informed consent was obtained from each volunteer prior to participation as approved by Children's Hospital, Boston, MA. The pedigree is of Irish-English descent and is depicted in Fig. 1. Male-to-male transmission indicated autosomal dominant inheritance. Genomic DNA was extracted from 5 mls of whole blood using standard protocols (Watts et al. 2004).

Clinical evaluation

The diagnosis of myopathy was based on proximal muscular weakness on physical examination and elevated serum creatine kinase activity, and in several individuals by EMG changes or muscle biopsy findings. Skeletal disease was identified by radiographic skeletal surveys including the skull, spine, hips, long bones, hands and feet, and measurement of serum alkaline phosphatase activity. Skin biopsy for collagen studies was obtained in the proband and was normal in the laboratory of Dr. Peter Byers, Collagen Diagnostic Laboratory, University of Washington Health Sciences Center, Seattle, WA.

Linkage analysis

DNA from 22 individuals underwent a genome-wide search at the National Heart, Lung, and Blood Institute Mammalian Genotyping Service (Marshfield, WI). A total of 402 microsatellite markers spanning the entire human genome were analyzed. All individuals included in the analysis were above 18 years of age. The disease was modeled as an autosomal dominant trait with age-dependent reduced penetrance. It was assumed that there were no phenocopies.

Lod score calculations

Four independent risk classes were identified and the estimated penetrance values were as follows: I, 0–18 years old, 0.01; II, 19–40 years old, 0.83; III, 41–45 years old, 0.90; and IV, >45 years, 0.95. Because the trait is rare, a disease allele frequency of 0.00001 was used in the analysis. Two-point linkage analysis was carried out using the MLINK program of the FASTLINK computer package (Cottingham et al. 1993). The marker-allele frequencies were estimated from the data by means of both observed

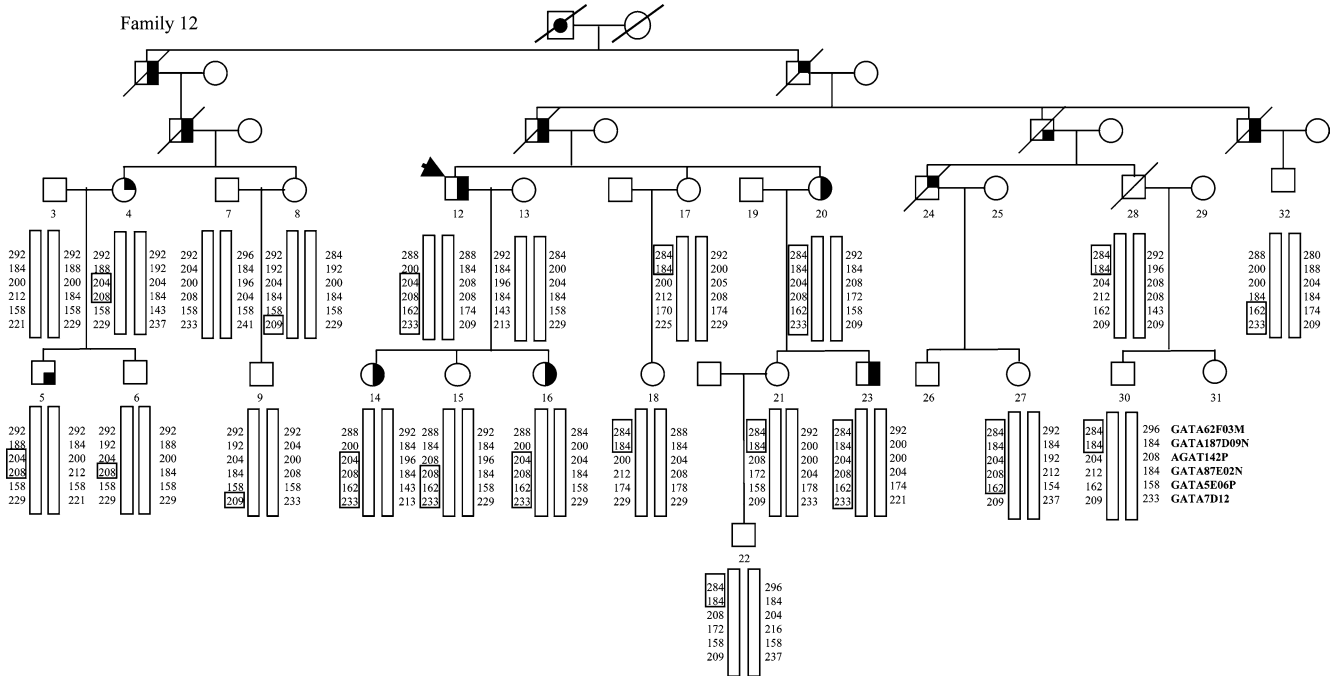

Fig. 1 Haplotype analysis in the pedigree. Individuals having muscle disease are denoted by *blackened*, *top-right*, *quarter symbols*; the bone disease is denoted by *blackened*, *bottom-right quarter*, *symbols*; males are denoted by *squares*; *circles* denote females; and a *diagonal line* through a symbol indicates deceased persons. Markers are listed from telomere (*top*) to centromere (*bottom*). The disease-linked haplotype is boxed

and reconstructed genotypes of founders within the pedigree. Sex-averaged genetic recombination maps were used to derive the intermarker distances. Genotypes were reconstructed where necessary. Linkage was considered established to a locus if an LOD score of at least +3 was obtained, and was considered excluded if an LOD score of less than −2 was found.

Mutation analysis

Primers for PCR amplification and subsequent sequencing of candidate genes TYRP1 and ADAMTL1 were designed using software at the Primer3 Web site (http://frodo.wi.mit.edu/cgi-bin/primer3/primer3_www.cgi) to flank all the exon–intron boundaries. PCR amplification, sequencing reactions, and mutation analysis were performed as described elsewhere (Watts et al. 2005).

Results

Clinical findings

Twenty-two living individuals (7 affected, 12 unaffected, and 3 spouses) representing three generations participated (Fig. 1). Clinical data was available for seven living affected subjects (three men and four women) as well as further clinical information for the six deceased affected individuals reported by Henry et al. (1958). In this family with limb-girdle myopathy, a distinctly unusual feature is fractures that precede the myopathy. Fractures are primarily of the long bones in the lower extremities, particularly the femora. Broken bones do not heal well leading to complications (in particular osteomyelitis resistant to treatment). Radiographs reveal coarse, sclerotic trabeculation with increased cortical thickening of the long bones and narrow medullary cavities (Fig. 2). Bone fragments taken recently from a fracture repair of the propositus were embedded without decalcification in methymethacrylate, sectioned, and stained with toluidine blue which highlights osteocytes (purple) and osteoid (blue bands). Some cortical bone fragments (Fig. 3a) showed irregularly shaped spaces filled with fibrous tissue, some lined by osteoid. Osteocytes within these areas were prominent and distributed unevenly. Other bone fragments (Fig. 3b) showed unremarkable cortical bone with a normal arrangement of osteons bearing a circular central canal, with a concentric array of surrounding small osteocytes. No large "Pagetoid" osteoclasts or cement (reversal) lines were present in this specimen to indicate Paget's disease of bone (PDB). Although osteomalacia-like changes in addition to infarction were previously reported in some individuals, this was not seen in this patient's specimen. Fractures had been slow to heal. Many individuals suffered osteomyelitis, which has been difficult to treat, leading to amputations in some cases.

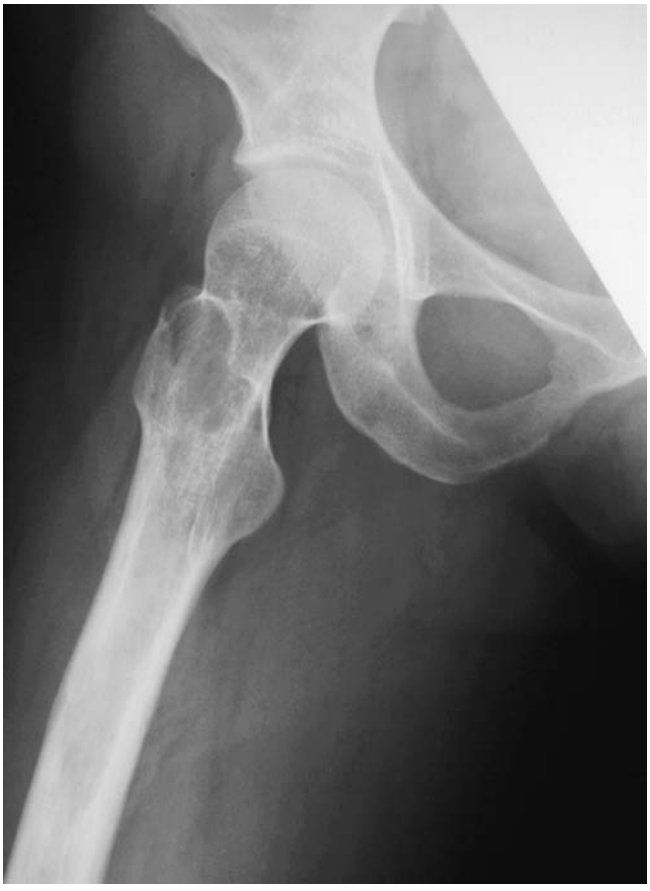

Fig. 2 Radiograph of the right hip of the proband shows coarse, sclerotic trabeculation with patchy cortical thickening and reduced medullary space affecting the femur

Locus mapping

As part of our overall approach to identify the genetic defect underlying this syndrome, exclusion linkage studies were undertaken in this multigenerational family to the LGMD and other myopathy loci (Mehta et al. 2005). The known bone disorders with overlapping pathological features, such as inclusion body myopathy, PDB and frontotemporal dementia (IBMPFD), Camurati-Engelmann disease (CED), familial expansile osteolysis, juvenile Paget's disease, and Kenny-Caffey disease were excluded by sequencing of the genes encoding VCP (valosin containing protein), TGFB1, RANK (*TNFRSF11A*), OPG (*TNFRSF11B*), and Sequestosome 1 (*SQSTM1*), and by the lack of distinctive radiological features of these conditions, respectively. A maximal LOD score (Z_{max}) of +3.74 was obtained with marker GATA87E02N, establishing linkage to chromosome 9p23-p21.1 for the pedigree (Table 1).

Haplotype analysis indicated that two markers, ATAG142P and GATA87E02N, were non-recombinant with the disease phenotype in the pedigree (Figs. 1, 4). Affected individuals 4, 5 and 12 define the telomeric boundary of the region by a recombination event

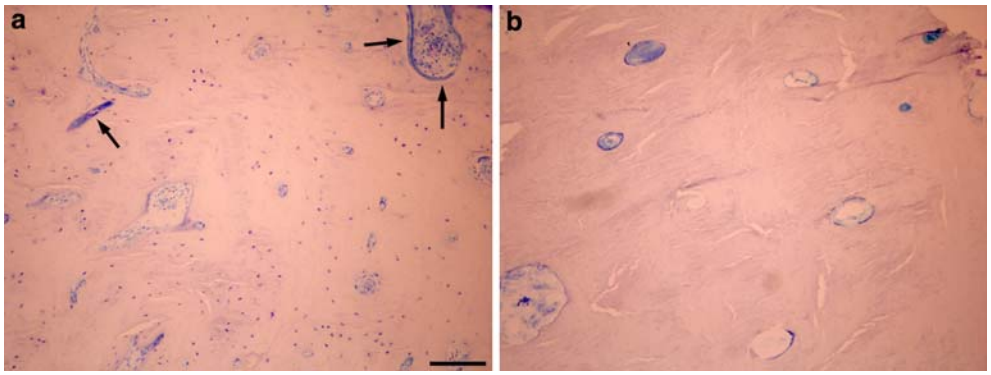

Fig. 3 Bone fragments from fracture repair were embedded without decalcification in methymethacrylate, sectioned, and stained with toluidine blue. Some fragments of cortical bone show irregularly shaped spaces filled with fibrous tissue, some lined by osteoid (*arrows*), and an uneven distribution of osteocytes (**a**). Other fragments represent unremarkable cortical bone, with a regular arrangement of a circular, central canal and surrounding small, inapparent osteocytes (**b**). *Scale bar* = 200 microns

Table 1 Family 12 pedigree: LOD scores with chromosome 9p markers

Marker (other names)	Marker position cM/Mb	LOD score at recombination fraction (θ)							Z_{max}	θ_{max}
		0.0	0.01	0.05	0.1	0.2	0.3	0.4		
GATA187D09N	21.9/10.22	−9.33	−1.86	−0.55	−0.09	0.18	0.19	0.10	0.19	0.300
AGAT142P	Unknown/17.26	1.01	1.19	1.41	1.40	1.13	0.74	0.35	1.47	0.075
GATA87E02 N (D9S1121)	44/25.39	3.74	3.67	3.41	3.07	2.35	1.56	0.76	3.74	0.000
GATA5E06P (D9S304)	58.3/32.31	−2.38	1.04	1.79	1.96	1.77	1.29	0.67	1.96	0.100
GATA7D12 (D9S301)	66/69.26	−1.83	1.37	1.80	1.75	1.36	0.91	0.46	1.80	0.050

between markers GATA187D09N and ATAG142P (Fig. 4a). A crossover between markers GATA87E02N and GATA5E06P that was observed in individuals 4 and 5 defined the centromeric boundary (Fig. 4b).

Accordingly, analysis of the pedigree suggests that the disease gene maps within a 36.4 cM interval between markers GATA187D09N and GATA5E06P. Based on the UC-Santa Cruz (Karolchik et al. 2003) sequence position, this region is approximately 22 Mb. The disease region could potentially be further refined between markers AGAT142P and GATA5E06P by crossovers in asymptomatic at-risk individuals, and would reduce the region to 15 Mb (Fig. 4c). Individuals 6, 15 and 27, who are at 50% risk of inheriting the disorder from an affected parent, currently do not display any feature of the disease, but have part of the disease haplotype (Fig. 4c), and may eventually help refine the critical region depending on their eventual disease status. Given the progressive nature of this syndrome, there is the potential to further refine the disease locus by crossovers in additional individuals in this family, and other families with similar features.

Candidate gene sequencing

This 9p21-p22 locus has been implicated in a number of cancer studies, suggesting several tumor-suppressing genes map to this region (Cannon-Albright et al. 1994; Harada et al. 1996; Mitelman 1994). Accordingly, two candidate genes are of particular interest given the phenotype of this disorder; ADAMTS-like 1 (ADAMTSL1) (Hirohata et al. 2002), and the tyrosinase-related protein 1 (TYRP1) (Abbott et al. 1991).

ADAMTSL1 (also known as punctin) is a member of the ADAMTS family of proteases responsible for extracellular matrix turnover (Tang 2001) and is highly expressed only in skeletal muscle. ADAMTSL1 is an especially intriguing candidate gene because another member of this family, ADAMTS13, which cleaves Von Willebrand factor is mutated in the clotting disorder Von Willebrand syndrome (Levy et al. 2001). However, we sequenced all 16 exons (coding and non-coding) of the three different splice forms of ADAMTSL1 in two affected individuals from the family. Only one silent base change (T to A) at position 3 of codon 51 in exon 2 was identified, which is a known SNP (rs2277160). Furthermore, this base change did not segregate with the disease. Similarly, for the tyrosinase-related protein 1 (TYRP1) gene, the 7 exons (coding and non-coding) were screened and no mutations or base changes were identified.

Discussion

Our genome-wide scan has identified the disease locus of progressive myopathy of a limb-girdle distribution and bone fragility to a 36.4 cM interval, mapping between markers GATA187D09N and GATA5E06P.

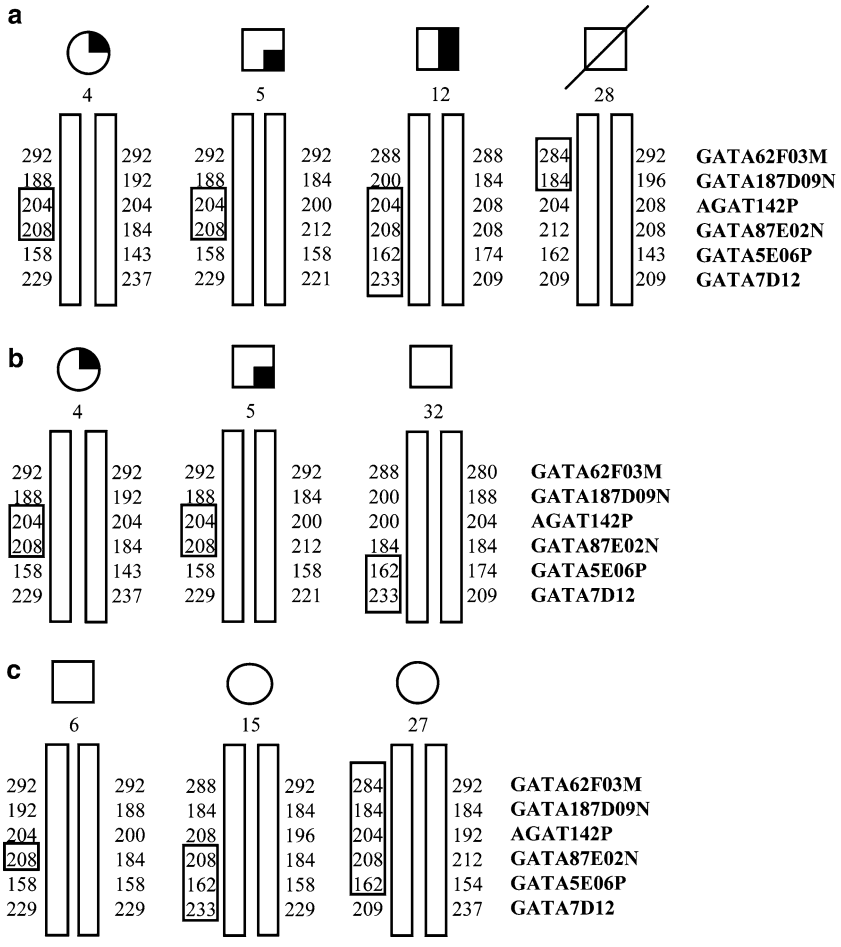

Fig. 4 Kindred haplotypes analyzed informative markers (GATA62FO3M, GATA187D09N, AGAT142P, GATA87E02N, GATA5E069 and GATA7D12) from the linkage region. Individual numberings are the same as in Fig. 1. Phenotypes of affected are identified by symbols. **a** Identification of the telomeric boundary. **b** Identification of the centromeric boundary. **c** Refinement of the telomeric boundary in asymptomatic at risk individuals

Notably, this chromosomal region contains the locus for diaphyseal medullary stenosis (DMS) with malignant fibrous histiocytoma (MFH) (MIM 112250; DMS-MFH), which has been mapped to chromosome 9p21-p22 between markers D9S1778 and D9S171 (Martignetti et al. 1999, 2000). However, the precise genetic defect is not known. This autosomal dominant, bone dysplasia/cancer syndrome features bone infarctions, cortical growth abnormalities, and pathological fractures. Approximately 35% of individuals affected with DMS develop MFH, which is a highly malignant bone sarcoma (Arnold 1973; Hardcastle et al. 1986). Clinical features for this disorder overlap with the skeletal problems of the family reported here (Table 2) and include pathological fractures with subsequent poor healing or non-union, progressive wasting and bowing of the legs, and painful debilitation. The bone dysplasia in both disorders typically presents during adolescence and is characterized by cortical growth abnormalities, including diffuse DMS with overlying endosteal cortical thickening and scalloping, metaphyseal striations, infarctions, and scattered sclerotic areas of the long bones. With DMS-MFH locus mapping to the progressive limb-girdle myopathy and bone fragility locus, this raises the possibility that these two disorders are allelic.

In this family's original clinical description (Henry et al. 1958), the gross histopathology of an irregular osteoporotic process with coarse trabeculation was reminiscent of PDB. From this initial and limited clinical data (six affected males), there were some features of PDB. In Table 2, we compare several bone disorders that have similar phenotypic and histological features. It is evident that there is overlap among all of these conditions, although the disorder investigated here has more bone features in common with DMS-MFH, but without malignant transformation. Similarly, Fig. 3 shows no large Pagetoid osteoclasts or cement lines indicative of classic PDB. Taken together, our findings suggest that this family does not have classic PDB and more likely represents a variation of DMS-MFH, especially given the fact that these two disorders have overlapping chromosomal loci.

Analysis in this region of two candidate genes, ADAMTSL1 and TYRP1, did not identify any disease mutations. Other interesting candidate genes that map on chromosome 9 within the critical region of this syndrome of hereditary progressive limb-girdle myopathy and bone fragility syndrome include Ras-related GTP binding A (RRAGA) (Schurmann et al. 1995), adipose differentiation-related protein (ADFP) (Eisinger and Serrero 1993), myeloid/lymphoid or mixed-lineage leu-

Table 2 Clinical profiles of IBMPFD, hereditary progressive limb-girdle myopathy and bone fragility syndrome, DMS-MFH, Camurati-Engelmann disease, and Kenny-Caffey syndrome

Phenotype	Disease				
	Limb-girdle myopathy and bone fragility	IBMPFD	DMS-MFH	Camurati- Engelmann	Kenny-Caffey
Bone dysplasia	X	X	X	X	–
Endosteal cortical thickening	X	X	X	–	–
Medullary stenosis	X	–	X	–	X
Bone infarctions	X	–	X	–	–
Pathologic fractures with poor healing	X	X	X	X	X
Malignant fibrous histiocytoma	–	–	X (35%)	–	–
Pre-senile cataracts	–	–	X (25%)	–	–
Proximal/distal muscle weakness	X	X	–	X	–
Premature hair graying	X	–	–	–	–
Clotting disorders	X	–	–	–	–
Thin skin	X	–	–	–	–
Craniofacial defects	–	–	–	–	X
Short stature	–	–	–	–	X
Hypoparathyroidism	–	–	–	–	X
Alkaline phosphatase	Low-normal	Elevated	Normal	Normal	Normal

kemia (MLLT3) (Nakamura et al. 1993), interferon gene cluster (Olopade et al. 1992), and methylthioadenosine phosphorylase (MTAP) (Nobori et al. 1996).

Discovery of the gene associated with hereditary, progressive limb-girdle muscular dystrophy and bone fragility syndrome will provide insight into the pathogenesis of muscle and bone disease revealing biological processes that control bone and muscle maintenance and regeneration.

Electronic-database information

Accession numbers and URLs for data in this article are as follows:

Online Mendelian Inheritance in Man (OMIM), http://www.ncbi.nlm.nih.gov.omim (for IBMPFD [MIM 167320], DMS-MFH [MIM 112250], Camurati Engelmann disease [MIM 131300], Kenny Caffey syndrome [MIM 244460])

Acknowledgements The authors thank the family for their participation, and thank their physicians for providing medical information and blood samples.

References

Abbott C, Jackson IJ, Carritt B, Povey S (1991) The human homolog of the mouse brown gene maps to the short arm of chromosome 9 and extends the known region of homology with mouse chromosome 4. Genomics 11:471–473

Arnold WH (1973) Hereditary bone dysplasia with sarcomatous degeneration: study of a family. Ann Intern Med 78:902–906

Cannon-Albright LA, Goldgar DE, Neuhausen S, Gruis NA, Anderson DE, Lewis CM, Jost M, Tran TD, Nyguen K, Kamb A, Weaver-Feldhaus J, Meyer LJ, Zone JL, Skolnick MH (1994) Localization of the 9p melanoma susceptibility locus (MLM) to a 2-cM region between D9S736 and D9S171. Genomics 23:265–268

Cottingham RWJ, Idury RM, Schaffer AA (1993) Faster sequential genetic linkage computations. Am J Hum Genet 53:252–563

Eisinger DP, Serrero G (1993) Structure of the gene encoding mouse adipose differentiation-related protein (ADRP). Genomics 16:638–644

Harada H, Hashimoto K, Ko MS (1996) The gene for multiple familial trichoepithelioma maps to chromosome 9p21. J Invest Dermatol 107:41–43

Hardcastle P, Nade S, Arnold WH (1986) Hereditary bone dysplasia with malignant change. J Bone Joint Surg 68A:1079–1089

Henry EW, Auckland NL, McIntosh HW, Starr DE (1958) Abnormality of the long bones and progressive muscular dystrophy in a family. Can Med Assoc J 78:331–336

Hirohata S, Wang LW, Miyagi M, Yan L, Seldin MF, Keene DR, Crabb JW, Apte SS (2002) Punctin, a novel ADAMTS-like molecule, ADAMTSL-1, in extracellular matrix. J Biol Chem 277:12182–12189

Karolchik D, Baertsch R, Diekhans M, Furey TS, Hinrichs A, Lu YT, Roskin KM, Schwartz M, Sugnet CW, Thomas DJ, Weber RJ, Haussler D, Kent WJ (2003) The UCSC genome browser database. Nucleic Acid Res 31:51–54

Levy GG, Nichols WC, Lian EC, Foroud T, McClintick JN, McGee BM, Yang AY, Slemieniak DR, Stark KR, Gruppo R, Sarode R, Shurin SB, Chandrasekaran V, Stabler SP, Sabio H, Bouhassira EE, Upshaw JD Jr, Ginsburg D, Tsai H-M (2001) Mutations in a member of the ADAMTS gene family cause thrombotic thrombocytopenic purpura. Nature 413:488–494

Martignetti JA, Desnick RJ, Aliprandis E, Norton KI, Hardcastle P, Nade S, Gelb BD (1999) Diaphyseal medullary stenosis with malignant fibrous histiocytoma: a hereditary bone dysplasia/cancer syndrome maps to 9p21–22. Am J Hum Genet 64:801–807

Martignetti JA, Gelb BD, Pierce H, Picci P, Desnick RJ (2000) Malignant fibrous histiocytoma: inherited and sporadic forms have loss of heterozygosity at chromosome bands 9p21–22-evidence for a common genetic defect. Gene Chromosome Canc 27:191–195

Mehta SG, Watts GD, Hamilton SJ, Wymer J, Mumm S, Whyte MP, McGillivray B, Kimonis VE (2005) Manifestations in a family with autosomal dominant bone fragility and linb-girdle myopathy. Am J Med Genet (in press)

Mitelman F (1994) Catalog of chromosome aberrations in cancer, 5 edn. Wiley/Liss, New York

Nakamura T, Alder H, Gu Y, Prasad R, Canaani O, Kamada N, Gale RP, Lange B, Crist WM, Nowell PC (1993) Genes on chromosomes 4, 9, and 19 involved in 11q23 abnormalities in acute leukemia share sequence homology and/or common motifs. Proc Natl Acad Sci USA 90:4631–4635

Nobori T, Takabayashi K, Tran P, Orvis L, Batova A, Yu AL, Carson DA (1996) Genomic cloning of methylthioadenosine phosphorylase: a purine metabolic enzyme deficient in multiple different cancers. Proc Natl Acad Sci USA 93:6203–6208

Olopade OI, Bohlander SK, Pomykala H, Maltepe E, Van Melle E, Le Beau MM, Diaz MO (1992) Mapping of the shortest region of overlap of deletions of the short arm of chromosome 9 associated with human neoplasia. Genomics 14:437–443

Schurmann A, Brauers A, Massmann S, Becker W, Joost HG (1995) Cloning of a novel family of mammalian GTP-binding proteins (RagA, RagBs, RagB1) with remote similarity to the Ras-related GTPases. J Biol Chem 270:28982–28988

Tang BL (2001) ADAMTS: a novel family of extracellular matrix proteases. Int J Biochem Cell Biol 33:33–44

Watts GD, Wymer J, Kovach MJ, Mehta SG, Mumm S, Darvish D, Pestronk A, Whyte MP, Kimonis VE (2004) Inclusion body myopathy associated with Paget disease of bone and fronto-temporal dementia is caused by mutant valosin-containing protein. Nat Genet 36:377–381